

Polar lipid remodeling and increased sulfatide expression are associated with the glioma therapeutic candidates, wild type p53 elevation and the topoisomerase-1 inhibitor, Irinotecan

Huan He · Carol L. Nilsson · Mark R. Emmett · Yongjie Ji · Alan G. Marshall · Roger A. Kroes · Joseph R. Moskal · Howard Colman · Frederick F. Lang · Charles A. Conrad

Received: 11 December 2008 / Revised: 10 March 2009 / Accepted: 29 May 2009 / Published online: 26 June 2009
© Springer Science + Business Media, LLC 2009

Abstract We report changes in gene and polar lipid expression induced by adenovirus-delivered wild-type (wt) p53 gene and chemotherapy of U87 MG glioblastoma cells, a treatment known to trigger apoptosis and cell cycle arrest. Sulfatides (sulfonated glycolipids) were most highly modulated by wild-type p53 treatment; however, no changes were observed in expression levels of mRNA for genes involved in sulfatide metabolism, indicating post-

transcriptional control of sulfatide synthesis. Modulation of the aglycones of GD1 and GM1b was observed in wild-type p53-treated cells. The treatment also leads to an increase in phospholipids such as phosphatidyl inositols, phosphatidyl serines, phosphatidyl glycerols, and phosphatidyl ethanolamines, especially hydroxylated phospholipids. These dramatic changes in the composition of cellular glycolipids in response to p53 gene expression and cytotoxic chemotherapy treatment indicate the large role that they play in cell signaling. The use of the human glioma cell line U87 appears to be an excellent model system both in tissue culture and in intracranial murine xenograft models to further characterize the role of sulfatides in modulating glioma responsiveness to therapeutic agents.

Electronic supplementary material The online version of this article (doi:10.1007/s10719-009-9249-6) contains supplementary material, which is available to authorized users.

H. He · C. L. Nilsson · M. R. Emmett · A. G. Marshall
National High Magnetic Field Laboratory,
Florida State University,
Tallahassee, FL 32310, USA

H. He · M. R. Emmett · A. G. Marshall
Department of Chemistry and Biochemistry,
Florida State University,
Tallahassee, FL 32306-4390, USA

R. A. Kroes · J. R. Moskal (✉)
Falk Center for Molecular Therapeutics,
Department of Biomedical Engineering, Northwestern University,
Evanston, IL, USA
e-mail: j-moskal@northwestern.edu

Y. Ji · H. Colman · F. F. Lang · C. A. Conrad
M.D. Anderson Cancer Center, Department of Neuro-oncology,
Houston, TX, USA

Present Address:
C. L. Nilsson
Pfizer Global Research and Development,
10770 Science Center Dr. (CB2),
San Diego, CA 92121, USA

Keywords Glioblastoma · Microarrays · Fourier transform ion cyclotron resonance mass spectrometry · Galectin-1 · Glycolipids · Phospholipids · Sulfatides · Lipidomics

Introduction

Despite recent advances in chemotherapy, radiation therapy and surgical intervention, malignant primary brain tumors such as glioblastoma, are nearly always fatal. The tumor cells are characterized by resistance to apoptosis and ability to invade surrounding normal tissue. The latter makes gross total surgical resections particularly difficult.

Lang *et al.* demonstrated that combined adenovirus transfection of wild-type p53 (wt p53) into glioma cell lines U87 and D54 followed by treatment with the

chemotherapeutic agent Irinotecan, an inhibitor of topoisomerase-1, or its metabolite SN-38 (7-ethyl-10-hydroxycamptothecin) triggered apoptosis and G2 arrest in the cells [1] and galectin-1 was found to be highly modulated by the therapy [2]. Knock-down of galectin-1 by siRNA in U87 cells led to a reduction in cell viability and increased sensitivity to SN-38; this result could be partially reversed by the addition of exogenous galectin-1 to the cell cultures. In xenograft mouse models of subcutaneous and intracranial implantation of U87 cells, the leading and invasive edges of both types of tumors expressed high levels of galectin-1 as determined by immunohistochemistry. The clinical relevance of these findings was confirmed by microarray analysis of clinical materials from patients with high-grade gliomas, demonstrating a positive correlation between increased galectin-1 expression and poor patient survival [2]. Taken together, the results indicate that galectin-1 may be a valuable therapeutic target to increase tumor cell sensitivity to cytotoxic agents and potentially reduce tumor invasiveness.

Galectin-1 is a protein that binds to epitopes that contain β -galactose in complex carbohydrate structures presented on glycolipids and glycoproteins. Galectin-1 may be found intracellularly or in the extracellular space as a homodimer. Intracellular galectin binds to H-Ras, a membrane protein that regulates cell proliferation, survival and death [3]. It has also been found that a mutant galectin-1 (L11A) can inhibit H-Ras [4]. Galectin-1 functions extracellularly to act as a cross-linking scaffold that binds cell surface glycoconjugates to the surface of other cells or to extracellular matrix molecules [5]. The cell-surface and lipid-raft associated ganglioside GM1 is known to be a major receptor for galectin-1 [6]. Cell density-dependent inhibition of growth and differentiation of neuroblastoma cells were associated with a ganglioside sialidase-mediated increase of GM1 and lactosylceramide on the cell surface [6].

Expression of wt p53 has been reported to be necessary for ceramide mediated apoptosis in leukemic cells [7]. Thus, it is possible that modulation of the expression of galectin-1 in glioblastoma cells by wt p53 may be associated with changes in the expression or distribution of glycolipids that expose galectin-1-binding glycoepitopes.

Glyco- and phospholipids are key actors in the decision of cellular fates such as apoptosis, cell cycle arrest or differentiation [8–12]. Glycosphingolipids (GSLs), often enriched in microdomains in the outer leaf of the plasma membrane, have been implicated as important adhesion and signaling molecules that mediate cellular “crosstalk” [13]. Tumor cells frequently express aberrant GSLs. Two carbohydrate antigens on cell surfaces, sialyl-Lewis^x and sialyl-Lewis^a, are considered to be promoters of tumor cell invasion [14]. Transfection of cells with glycosyltransferase

genes has been demonstrated to modulate cellular fate in tumor cells [15–18].

Phospholipids, once considered to be strictly structural components of the cell membrane, are now known to form an important substrate pool for the production of second messenger molecules [11, 19, 20]. Phosphorylated metabolites of phosphatidyl inositol may be formed by the activation of phosphoinositide kinases, which are in turn controlled by cell surface receptors. The intracellular levels of inositol 3,4-bisphosphate and inositol 3,4,5-triphosphate are involved in the control of cell survival, proliferation and movement [11].

The purpose of the studies reported here was to further evaluate the regulation of the expression of galectin-1 by investigating changes in glycogene and polar lipid expression in U87 cells in response to wt p53 or empty vector therapy, followed by treatment with SN-38 by use of a recently developed approach targeted to polar lipids in U87 cells, including complex glycolipids such as gangliosides in addition to phospholipids [21]. The method permits facile distinction between aglycones of variable compositions, as well as the polar carbohydrate head groups. Most of the existing literature has focused on a subset of lipids in each study, such as phospholipids and smaller glycolipids (*i.e.*, glucosyl ceramides) [19, 22–24] or larger glycolipids (gangliosides) [25]. Concomitant measurements of both types of lipid may present a broader picture of how tumor cell membranes change in response to stimulation such as gene therapy or pharmacological agents. Transcriptome analysis of the human glycome was also performed in an attempt to correlate gene expression changes with alterations in glycolipid changes following wt p53 infection of U87 cells.

Materials and methods

Cell culture The glioma cell line U87 MG (ATCC #HTB-14) was grown in the presence of DMEM-F12 media supplemented with 10% FBS (Cell Gro, Mediatech, Herndon, VA) in a humidified CO₂ incubator at 5% CO₂. Cell cultures were grown in 150-mm dishes to 90% confluency.

Treatment of cells Cells ($\sim 2 \times 10^6$) were treated with adenoviruses (therapeutic Ad-p53 or D1-312 control adenovirus vector) or cytotoxic chemotherapy (SN-38), either alone, in combination or in different sequences. Cell cultures were treated for 24 h with SN-38 at a final concentration of 0.1 μ M (stock solution of 10 mM). Cell cultures were also treated with either control virus D1-312 or test virus that contained wild-type p53 gene inserted in the E1 region of the adenovirus vector (Ad-p53) at 1:100

MOI (multiplicity of infection) from a stock virus titrated at 2.8×10^{11} pfu (plaque-forming units). Cell cultures that were treated with a combination of drug and virus included a total incubation period of 48 h allowing 24 h for each agent. Cells were washed three times with room-temperature phosphate-buffered saline between treatments. Prior to viral infection, the cells were placed in serum-free media for 1 h to ensure adequate absorption of virus to the cells.

Glycotranscriptomic analysis The techniques for microarray fabrication, target preparation, data acquisition and statistical analysis have been described in detail [26]. Briefly, the 359 genes comprising our focused Human Glycobiology microarray are compiled from currently available NCBI/EMBL/TIGR human sequence databases and the Consortium for Functional Glycomics-CAZy databases (available at www.cazy.org/CAZY/) and represent all of the cloned human glycosyltransferases, glycosylhydrolases, polysaccharide lyases, and carbohydrate esterases. Individual 45-mer oligonucleotides complementary to sequences within these human mRNAs along with control oligonucleotides representing the most traditionally-accepted and commonly-utilized housekeeping genes [27] were designed and prioritized according to stringent selection criteria [ArrayDesigner v2.03]. These optimal oligonucleotides were individually synthesized with the addition of a 5'-amino linker (C6-TFA, Glen Research) onto each oligonucleotide, then robotically arrayed and covalently linked in quadruplicate to aldehyde-coated glass microscope slides, and quality controlled prior to use. Total RNA was extracted from tissues with guanidine isothiocyanate and CsCl-ultracentrifugation, purified (Qiagen) and used as the substrate for RNA amplification and labeling, exactly as described [26]. We utilized universal human reference RNA (Stratagene) in our analyses and treated identical aliquots concurrently with the tissue samples. Equivalent amounts of Cy5-labeled (experimental) and purified Cy3-labeled (reference) amplified RNA (aRNA) targets (each labeled to 15–18% incorporation) were combined, denatured and hybridized at 46°C for 16 h. Following sequential high stringency washes, individual Cy3 and Cy5 fluorescence hybridization to each spot on the microarray was quantitated by a high resolution confocal laser scanner. Arrays were scanned (at 633 nm & 543 nm) at 5 micron resolution on the ScanArray 4000XL (Packard Biochip Technologies) utilizing QuantArray software [v3.0] at the maximal laser power that produced no saturated spots. The adaptive threshold method was used to differentiate the spot from the background and spot intensity determined from median pixel intensity. Prior to normalization, eight individual quality confidence measurements were calculated for each scanned array and spots were

flagged that did not pass stringent selection criteria. The data from each channel were normalized by use of the LOWESS curve-fitting equation on a print-tip specific basis (GeneTraffic v2.8, Iobion Informatics).

Polar lipid extraction Cells ($\sim 2 \times 10^6$) were extracted by the addition of methanol:chloroform 1:1 and sonicated for 30 min. The extract was incubated overnight at 48°C in order to optimize GSL yields. After centrifugation, the supernatant was collected and partitioned with additional chloroform and H₂O. The upper layer was collected and dried. Approximately 1/50th of the total extract was consumed per LC-MS experiment.

nanoLC-MS The lipids were reconstituted in 80% methanol (aq) with the addition of 10 mM NH₄OAc and separated by nano-liquid chromatography (Eksigent) in a self-packed 80 mm \times 50 μ m phenyl-hexyl column (Phenomenex, Torrance, CA). The gradient was 15%/85% to 2%/98% A/B during 4 min (Solvent A: 98% H₂O, 2% methanol, and 10 mM NH₄OAc; B: 98% methanol, 2% H₂O, 10 mM NH₄OAc) with a flow rate of 400 nL/min. LC effluent was analyzed on-line by negative-ion micro-electrospray and a modified hybrid linear ion trap FT-ICR MS equipped with a 14.5 T magnet [28]. Precursor ion mass spectra were collected at high mass resolving power ($m/\Delta m_{50\%} = 200,000$ at m/z 400) and scan rate (>1 Hz). The instrument was calibrated with a mixture (ESI calibration solution, Thermo Fisher) according to the manufacturer's recommendation. Typical broadband external calibration mass accuracy is better than 500 ppb. Data-dependent MS/MS was performed in the linear ion trap (collisional dissociation) during collection of the ICR time-domain data [21].

Results

Lipidomic analysis Approximately 1/50th of the polar lipid fraction of the cell extract ($\sim 2 \times 10^6$ cells) was separated by nano-liquid chromatography (nanoLC) to resolve polar lipids based on variations of polar head group (e.g., oligosaccharides in glycolipids or phosphorylated end groups in phospholipids) and the hydrophobic lipid tails (ceramides in glycolipids or diacyl glycerol in phospholipids). Separation prior to MS detection of a complex mixture of components with different ionization efficiency and/or abundance will improve the sensitivity and quantification linearity. Signal magnitude and accurate mass measurement of the precursor ions from the nanoLC effluent were acquired with our 14.5 T FT-ICR mass spectrometer [28]. Accurate mass (typically better than 500 ppb), isotope ratios, nanoLC retention time trends,

along with available tandem mass spectra generated from collisional induced dissociation (CID) of precursor ions in the linear ion trap (LTQ) enable structural assignment of hundreds of lipid species [21]. Average signal magnitudes from duplicate nanoLC-MS experiments were calculated to reflect the abundance of lipid species in the cell samples.

We observed five sulfatides (Fig. 1), of which four contained short chain ceramides, *i.e.*, (34:1), (34:1) + O, (34:2) and (34:2) + O. The only observed long chain-containing sulfatide was (42:2). Treatment of cells with a combination of p53 and SN38 in either order resulted in a dramatic increase in short chain sulfatide levels. In contrast, short chain sulfatides were barely detectable in cells treated with wt p53 alone, SN-38 alone, empty vector DI-312 or untreated cells. In addition, the order of administration of wt p53 and SN-38 significantly affected the short chain sulfatide levels. Cells treated with wt p53 followed by SN-38 showed an approximately 2-fold greater increase in short chain sulfatides than cells treated in reverse order. For the long chain sulfatide, again, the highest level was present in cells treated with wt p53 followed by SN-38. However, such treatment brought only a moderate increase (less than 2-fold) in long chain sulfatide level compared to control cells (treated with empty adenoviral vector DI-312 followed by SN-38). Similar to short chain sulfatides, the long chain sulfatides level dramatically increased in cells treated with SN-38 followed by p53 compared to control cells (treated with SN-38 followed by empty vector DI-312).

We detected 32 gangliosides (Fig. 2), including 13 GM3, 4 GM2 α , 8 GM1b, 1 asialo-GM1 and 6 GD1. The most significant change was the decrease of long chain gangliosides, especially GD1 and GM1b, in cells treated with wt p53 followed by SN-38 compared to control cells (treated with empty adenoviral vector DI-312 followed by SN-38). No detectable change in ganglioside profile was observed in other wt p53 treated cells, either with wt p53 alone or in reverse order (SN-38 followed by wt p53), compared to the corresponding empty vector DI-312 treated cells.

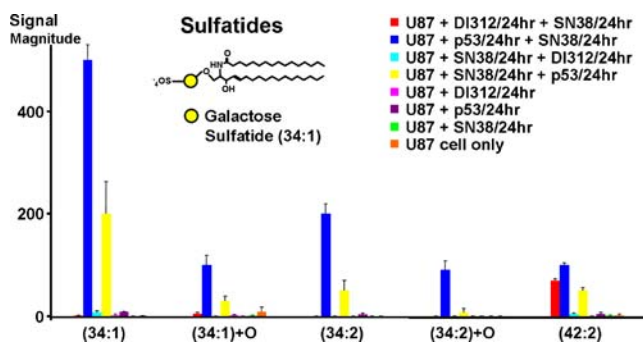


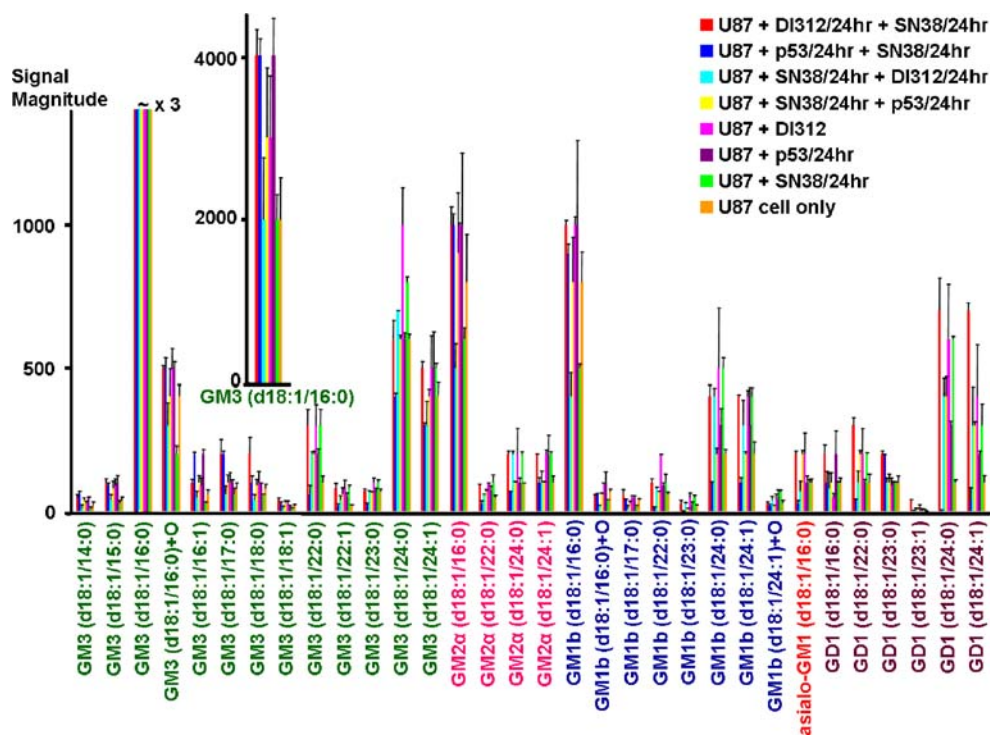
Fig. 1 Sulfatide composition in U87 MG cells following various gene and/or chemotherapy treatments

However, reversed order treatment resulted in increased level of long chain gangliosides, especially GD1 and GM1b (SN-38 followed by wt p53 compared to wt p53 followed by SN-38).

We observed four subclasses of phospholipids, including 55 phosphatidyl inositols (PI), 51 phosphatidylserines (PS), 10 phosphatidylethanolamines (PE), and 14 phosphatidylglycerols (PG) (Fig. 3). Because all four subclasses of phospholipids followed similar trends, only modulation of PG levels is shown. Increase in PG level was observed in all wt p53 treated cells (with wt p53 alone or in combination with SN-38 in either order) compared to the corresponding empty adenoviral vector DI-312 treated cells. The most noteworthy increase in PG, especially hydroxylated PG, was found in cells treated with wt p53 followed by SN-38 compared to control cells (DI-312 followed by SN-38). PG levels decreased when administration order of wt p53 and SN38 was reversed (SN-38 followed by wt p53 compared to wt p53 followed by SN-38).

Glycotranscriptomic analysis We compared the expression of 359 glyco-related genes with our in-house fabricated focused oligonucleotide microarray platform of SN-38-treated U87 cells in the presence or absence of p53 expression to untreated parental U87 cells. RNA samples were studied in triplicate (three microarray slides for each sample). Each oligonucleotide was spotted in quadruplicate on the array, for a total of 12 expression measurements for each gene in each group. We employed a universal reference design [29] and comprehensive statistical analysis platforms to facilitate acquisition of expression profiles. We used Significance Analysis of Microarrays (SAM) analysis to determine statistically significant differences in the measured expression levels for each gene on the array [26] and demonstrated that a number of genes could be identified with high confidence as differentially expressed between the compared cell types. Table 1 shows the identities, functional annotations, and relative expression ratios of these differentially expressed genes in samples treated with wt p53 before treatment with SN-38. Of the 359 genes, 20 glyco-genes differed in their expression between treated and untreated cells by at least 1.2-fold at a 0% False Discovery Rate (FDR). Importantly, at this stringent FDR, none of these changes was expected to be a false positive. Of the 20 genes, 16 had increased and 4 had decreased measured expression levels in cells treated with wt p53 followed by SN-38 compared to untreated U87 cells. The differentially expressed transcripts fell into well-defined pathways for glycan biosynthesis and metabolism [30], including N-glycan biosynthesis and degradation, O-glycan biosynthesis, and neo-lactoseries blood group glycolipid biosynthesis.

Fig. 2 Ganglioside compositions in U87 MG cells following various gene and/or chemotherapy treatments



Similarly, Table 2 shows the identities, functional annotations, and relative expression ratios of these differentially expressed genes when the order of treatment is reversed. Of the 359 glyco genes analyzed, 18 genes differed in their expression between treated and non-treated cells by at least 1.2-fold, based on the most stringent statistical criteria. Of

these 18 genes, 10 had increased and 8 had decreased measured expression levels in the cells treated with SN-38 followed by wt p53 compared to untreated U87 cells. In addition to genes involved in N- and O-glycan biosynthesis, genes responsible for lactoseries blood group glycolipid biosynthesis and GPI-anchor biosynthesis were also affected.

Fig. 3 Phosphatidylglycerol compositions in U87 MG cells following various gene and/or chemotherapy treatments

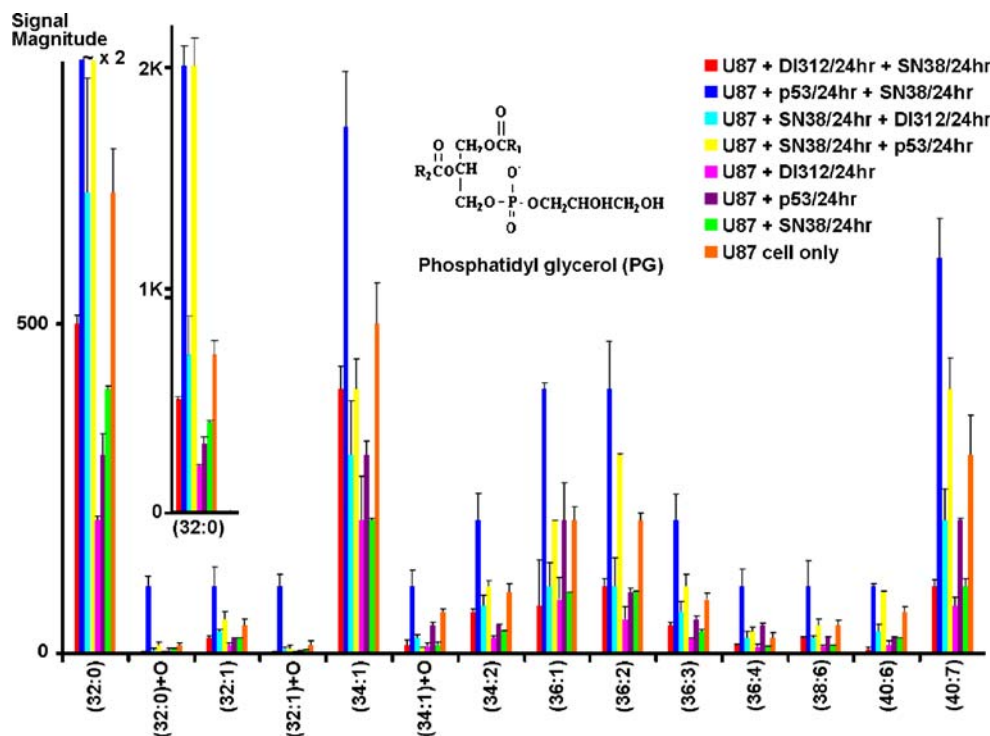


Table 1 Comparative transcriptomic changes for U87 MG cells treated with Ad-p53 for 24 h and SN-38 for 24 h vs. untreated U87 MG cells

GENBANK Accession	Fold change ^a	Gene ID
<i>Glycogenes</i>		
<i>N-GLYCAN BIOSYNTHESIS</i>		
NM_002406	1.90	MANNOSYL (α 1,3-)-GLYCOPROTEIN β 1,2- <i>N</i> -ACETYLGLUCOSAMINYLTRANSFERASE
NM_004480	1.46	FUCOSYLTRANSFERASE 8 (α 1,6 FUCOSYLTRANSFERASE)
NM_173540	1.24	FUCOSYLTRANSFERASE 11 (α 1,3 FUCOSYLTRANSFERASE)
NM_002372	-1.26	α -MANNOSIDASE, CLASS 2A, MEMBER 1
<i>N-GLYCAN DEGRADATION</i>		
NM_000434	1.43	SIALIDASE 1 (LYSOSOMAL SIALIDASE)
NM_000147	1.38	FUCOSIDASE, α -L-1
NM_000404	1.27	β 1-GALACTOSIDASE
<i>O-GLYCAN BIOSYNTHESIS</i>		
NM_018414	4.20	ST6 (α - <i>N</i> -ACETYL-NEURAMINYL-2,3- β -GALACTOSYL-1,3)- <i>N</i> -ACETYL GALACTOSAMINIDE α -2,6 SIALYL-TRANSFERASE 1
NM_022087	1.54	UDP- <i>N</i> -ACETYL- α -D-GALACTOSAMINE:POLYPEPTIDE <i>N</i> -ACETYL GALACTOSAMINYLTRANSFERASE 11 (GALNAC-T11)
AF154107	1.37	UDP- <i>N</i> -ACETYL- α -D-GALACTOSAMINE:POLYPEPTIDE <i>N</i> -ACETYL GALACTOSAMINYLTRANSFERASE 5 (GALNAC-T5)
NM_017423	-1.57	UDP- <i>N</i> -ACETYL- α -D-GALACTOSAMINE:POLYPEPTIDE <i>N</i> -ACETYL GALACTOSAMINYLTRANSFERASE 7 (GALNAC-T7)
NM_152692	-1.77	C1GALT1-SPECIFIC CHAPERONE 1
<i>BLOOD GROUP GLYCOLIPID BIOSYNTHESIS-NEO-LACTOSERIES</i>		
NM_014256	1.49	UDP-GlcNAc: β GAL β 1,3- <i>N</i> -ACETYLGLUCOSAMINYLTRANSFERASE 3
<i>KERATIN SULFATE BIOSYNTHESIS</i>		
NM_145236	1.66	UDP- GlcNAc: β GAL β 1,3- <i>N</i> -ACETYLGLUCOSAMINYLTRANSFERASE 7
<i>CHONDROITIN SULFATE BIOSYNTHESIS</i>		
NM_012200	1.48	β 1,3-GLUCURONYLTRANSFERASE 3 (GLUCURONOSYLTRANSFERASE I)
<i>LIPOPOLYSACCHARIDE BIOSYNTHESIS</i>		
BC039145	2.19	GLYCOSYLTRANSFERASE 8 DOMAIN CONTAINING 3
NM_018446	1.40	GLYCOSYLTRANSFERASE 8 DOMAIN CONTAINING 1
<i>STARCH AND SUCROSE METABOLISM</i>		
NM_002863	1.56	GLYCOGEN PHOSPHORYLASE (HERS DISEASE, GLYCOGEN STORAGE DISEASE TYPE VI)
NM_015831	1.35	ACETYLCHOLINESTERASE (YT BLOOD GROUP)
NM_000158	-3.32	GLUCAN (1,4- α -), BRANCHING ENZYME 1
<i>Housekeeping/Control Genes</i>		
NM_000930	2.23	TISSUE PLASMINOGEN ACTIVATOR
NM_001069	2.13	β 2A-TUBULIN
NM_005345	1.75	HEAT SHOCK 70KDA PROTEIN 1A
NM_001540	1.60	HEAT SHOCK 27KDA PROTEIN 1
NM_000447	1.57	PRESENILIN 2 (ALZHEIMER DISEASE 4)
NM_007096	1.55	CLATHRIN, LIGHT POLYPEPTIDE (LCA)
NM_000942	1.54	PEPTIDYLPROLYL ISOMERASE B (CYCLOPHILIN B)
NM_001266	1.49	CARBOXYLESTERASE 1 (MONOCYTE/MACROPHAGE SERINE ESTERASE 1)
NM_173090	1.37	CALPAIN 3, (P94)
BC014495	1.37	RADICAL FRINGE HOMOLOG (DROSOPHILA)
NM_003472	-2.65	DEK ONCOGENE (DNA BINDING)
NM_006082	-2.28	α -TUBULIN
NM_000194	-2.01	HYPOXANTHINE PHOSPHORIBOSYLTRANSFERASE 1 (LESCH-NYHAN SYNDROME)
NM_003380	-1.75	VIMENTIN
AF112219	-1.74	ESTERASE D/FORMYLGLUTATHIONE HYDROLASE

Table 1 (continued)

GENBANK Accession	Fold change ^a	Gene ID
U93051	-1.70	PHOSPHATASE AND TENSIN HOMOLOG (MUTATED IN MULTIPLE ADVANCED CANCERS 1)
NM_005348	-1.65	HEAT SHOCK PROTEIN 90KDA ALPHA (CYTOSOLIC), CLASS A MEMBER 1
NM_001428	-1.56	α -ENOLASE 1
NM_002156	-1.49	HEAT SHOCK 60KDA PROTEIN 1 (CHAPERONIN)
NM_002629	-1.32	PHOSPHOGLYCERATE MUTASE 1 (BRAIN)

Positive values indicate an increase, and negative a decrease, in gene expression in U87 + P53/24hr + SN38/24hr relative to U87

^a The fold change was calculated between mean values of U87 + P53/24hr + SN38/24hr ($n=3$) and U87 ($n=3$) tissue

Ontological analyses To identify other genes and globally affected pathways involved in treatment-dependent transcriptome responses, we utilized Gene Set Enrichment Analysis (GSEA) as an adjunct to our comprehensive glycoexpression analysis. GSEA extends the interpretation of large scale experiments from the identification of single genes to the identification of pathways and processes, and focuses on gene sets that tend to be more reproducible and interpretable. Single gene methods are powerful only when the individual gene effect is marked and the variance is small across samples, unlikely in complex drug responses. GSEA considers all of the genes in an experiment rather than only those above an arbitrary cutoff in terms of fold-change or significance. Such analyses are instrumental if complex phenotypes result from modest variation in the expression or activity of multiple members of a given pathway. As such, GSEA provides additional statistical rigor to discriminate those additional genesets modified in complex diseases from the datasets even when individual genes do not demonstrate significance. Because the single-gene analyses revealed only modest changes and did not illuminate globally affected pathways, a GSEA was performed. GSEA has been applied widely as a tool for such gene-set analyses [31–34]. Altogether, 3 such regulated pathways emerged in the analysis according to the criteria (NOM p-value < 0.01 and False Discovery Rate $q < 0.25$) recommended by Subramanian *et al.* [33]. A complete list of significantly affected pathways for each treatment regimen is provided in Table 3.

GSEA analysis demonstrated significant enrichment in genes related to O-glycan biosynthesis in SN38-treated cell cultures irrespective of the p53 background, and thus appeared to be due to drug treatment alone (Table 3 and Fig. 4). GSEA analysis also identified two gene sets uniquely associated with the time of delivery of wt p53, namely genes related to glycerolipid metabolism and blood group glycolipid biosynthesis lacto-series.

Genes related to O-glycan biosynthesis were enriched in both groups. The individual genes comprising these gene sets are depicted in Fig. 4, along with the expression profiles of the individual genes within each gene set that contribute to the normalized enrichment score. Moreover, the subset of genes within the gene set that are primarily responsible for the statistically significant enrichment of these gene sets (*i.e.*, those comprising the leading edge of the gene set) are also highlighted in Fig. 4.

Discussion

NanoLC-micro-ESI coupled to high-field FT-ICR mass spectrometry [28, 35, 36] led to the detection, resolution, and assignment of hundreds of m/z species in the polar lipid extracts from glioma cells. In many instances, MS/MS data obtained from ion trap dissociation of molecular ions confirmed precursor ion identities. NanoLC separation was determined to be essential in order to detect and measure the molecules in a complex mixture. Unlike immunological-based methods, nanoLC-MS/MS can determine both the structure of the polar head and lipid composition of glyco- and phospholipids, allowing for a more complete description of molecular changes in a cell.

Glyco- and phospholipids are known to associate with signal transduction protein mediators. The discovery of modulation of galectin-1 by wt p53 in glioma cells encouraged us to examine changes in the lipidome, because GM1 is a major ligand of galectin-1 [6]. Sulfatides are ligands for other galectins [37]. Phospholipids are known to form a substrate pool for the production of second messenger molecules [20]. Phosphorylated metabolites of phosphatidylinositol, such as inositol 3,4-bisphosphate and inositol 3,4,5-triphosphate, are involved in the control of cell survival, proliferation and movement [11, 38]. Binding of phosphatidylserine by annexin-V on the surface of

Table 2 Comparative transcriptomic changes for U87 MG cells treated with SN-38 for 24 h and Ad-p53 for 24 h vs. untreated U87 MG cells

GENBANK Accession	Fold change ^a	Gene ID
<i>Glycogenes</i>		
<u><i>N-GLYCAN BIOSYNTHESIS</i></u>		
NM_002406	1.46	MANNOSYL (α 1,3-)-GLYCOPROTEIN β 1,2- <i>N</i> -ACETYLGLUCOSAMINYLTRANSFERASE
NM_033087	1.38	ASPARAGINE-LINKED GLYCOSYLATION 2 HOMOLOG (α 1,3-MANNOSYLTRANSFERASE)
NM_014275	-2.23	MANNOSYL (α 1,3-)-GLYCOPROTEIN β 1,4- <i>N</i> -ACETYLGLUCOSAMINYLTRANSFERASE, ISOZYME B, transcript variant 1
NM_054013	-1.58	MANNOSYL (α 1,3-)-GLYCOPROTEIN β 1,4- <i>N</i> -ACETYLGLUCOSAMINYLTRANSFERASE, ISOZYME B, transcript variant 2
NM_002372	-1.36	α -MANNOSIDASE, CLASS 2A, MEMBER 1
NM_144988	-1.34	ASPARAGINE-LINKED GLYCOSYLATION 14 HOMOLOG (YEAST)
<u><i>O-GLYCAN BIOSYNTHESIS</i></u>		
NM_018414	2.52	ST6 (α - <i>N</i> -ACETYL-NEURAMINYL-2,3- β -GALACTOSYL-1,3)- <i>N</i> -ACETYL GALACTOSAMINIDE α -2,6 SIALYL-TRANSFERASE 1
NM_022087	1.59	UDP- <i>N</i> -ACETYL- α -D-GALACTOSAMINE:POLYPEPTIDE <i>N</i> -ACETYL GALACTOSAMINYLTRANSFERASE 11 (GALNAC-T11)
NM_017423	-1.69	UDP- <i>N</i> -ACETYL- α -D-GALACTOSAMINE:POLYPEPTIDE <i>N</i> -ACETYL GALACTOSAMINYLTRANSFERASE 7 (GALNAC-T7)
NM_152692	-1.28	C1GALT1-SPECIFIC CHAPERONE 1
<u><i>BLOOD GROUP GLYCOLIPID BIOSYNTHESIS-NEO-LACTOSERIES</i></u>		
NM_000149	-1.67	FUCOSYLTRANSFERASE 3 (GALACTOSIDE 3(4)-L-FUCOSYLTRANSFERASE, LEWIS BLOOD GROUP)
<u><i>GLOBOSIDE METABOLISM</i></u>		
NM_017436	1.72	α 1,4-GALACTOSYLTRANSFERASE (GLOBOTRIAOSYLCERAMIDE SYNTHASE)
<u><i>GLYCOSYLPHOSPHATIDYLINOSITOL(GPI) ANCHOR BIOSYNTHESIS</i></u>		
NM_145167	1.57	PHOSPHATIDYLINOSITOL GLYCAN, CLASS M
<u><i>LIPOPOLYSACCHARIDE BIOSYNTHESIS</i></u>		
BC039145	2.02	GLYCOSYLTRANSFERASE 8 DOMAIN CONTAINING 3
<u><i>STARCH AND SUCROSE METABOLISM</i></u>		
NM_012200	1.45	β 1,3-GLUCURONYLTRANSFERASE 3 (GLUCURONOSYLTRANSFERASE I)
NM_000028	1.42	AMYLO-1, 6-GLUCOSIDASE, 4- α -GLUCANOTRANSFERASE
NM_004130	1.29	GLYCOGENIN 1
NM_000158	-2.94	GLUCAN (1,4- α -), BRANCHING ENZYME 1
<u><i>Housekeeping/Control Genes</i></u>		
NM_000930	2.47	TISSUE PLASMINOGEN ACTIVATOR
NM_001069	2.02	β 2A-TUBULIN
NM_005324	1.53	H3 HISTONE, FAMILY 3A
NM_006572	1.47	GUANINE NUCLEOTIDE BINDING PROTEIN (G PROTEIN), α 13
NM_019593	1.30	HYPOTHETICAL PROTEIN KIAA1434
NM_001540	1.30	HEAT SHOCK 27KDA PROTEIN 1
NM_018136	-2.34	HYPOTHETICAL PROTEIN FLJ10517
NM_003472	-1.79	DEK ONCOGENE (DNA BINDING)
AF112219	-1.73	ESTERASE D/FORMYLGLUTATHIONE HYDROLASE
NM_006082	-1.68	α -TUBULIN
NM_003380	-1.67	VIMENTIN
NM_000194	-1.58	HYPOXANTHINE PHOSPHORIBOSYLTRANSFERASE 1 (LESCH-NYHAN SYNDROME)
U93051	-1.52	PHOSPHATASE AND TENSIN HOMOLOG (MUTATED IN MULTIPLE ADVANCED CANCERS 1)
NM_002205	-1.42	α 5-INTEGRIN, (FIBRONECTIN RECEPTOR, α POLYPEPTIDE)
NM_001428	-1.38	α -ENOLASE 1
NM_001537	-1.29	HEAT SHOCK FACTOR BINDING PROTEIN 1

Positive values indicate an increase, and negative a decrease, in gene expression in U87 + SN38/24hr + P53/24hr relative to U87

^a The fold change was calculated between mean values of U87 + SN38/24hr + P53/24hr ($n=3$) and U87 ($n=3$) tissue

Table 3 Significantly enriched pathways identified by gene set enrichment analysis (GSEA)

Treatment	Pathway name	Source	Size	ES	NES	NOM p-value	FDR q-value
p53/SN-38	O-glycan biosynthesis	KEGG	17	0.581	1.699	0.0078	0.0370
	glycolipid biosynthesis-lactoseries	KEGG	9	-0.687	-1.671	0.0038	0.0488
	glycerolipid metabolism	KEGG	4	0.772	1.419	0.0484	0.2277
SN-38/p53	O-glycan biosynthesis	KEGG	20	0.543	1.634	0.0060	0.0960

ES enrichment score, NES normalized enrichment score, NOM nominal, FDR false discovery rate

apoptotic glioma cells can inhibit phagocytosis by microglia [39]. Recent studies also suggest that natural lectins secreted by cells can modulate lipid raft organization, block co-stimulatory-dependent lipid raft migration to T-cell/antigen presenting cell contact sites, and alter T-cell activation. In fact, galectin-4, a major member of the galectin family, has been suggested to be an organizer of lipid rafts [40]. In addition, both galectin-1 and galectin-8 have been identified by detailed proteomic analysis of human monocyte proteins associated with lipid rafts [41]. It has been proposed that galectin-1 directly interferes with protein segregation and lipid raft reorganization in immunoregulatory T-cells [42]. However, it remains to be determined whether galectin-1 can likewise organize/reorganize lipid rafts on the glioma cell surface. In support of this possibility, galectin-1 has been recently implicated in mediating the PKC ϵ -vimentin controlled integrin β 1 membrane recycling pathway in glioma [43].

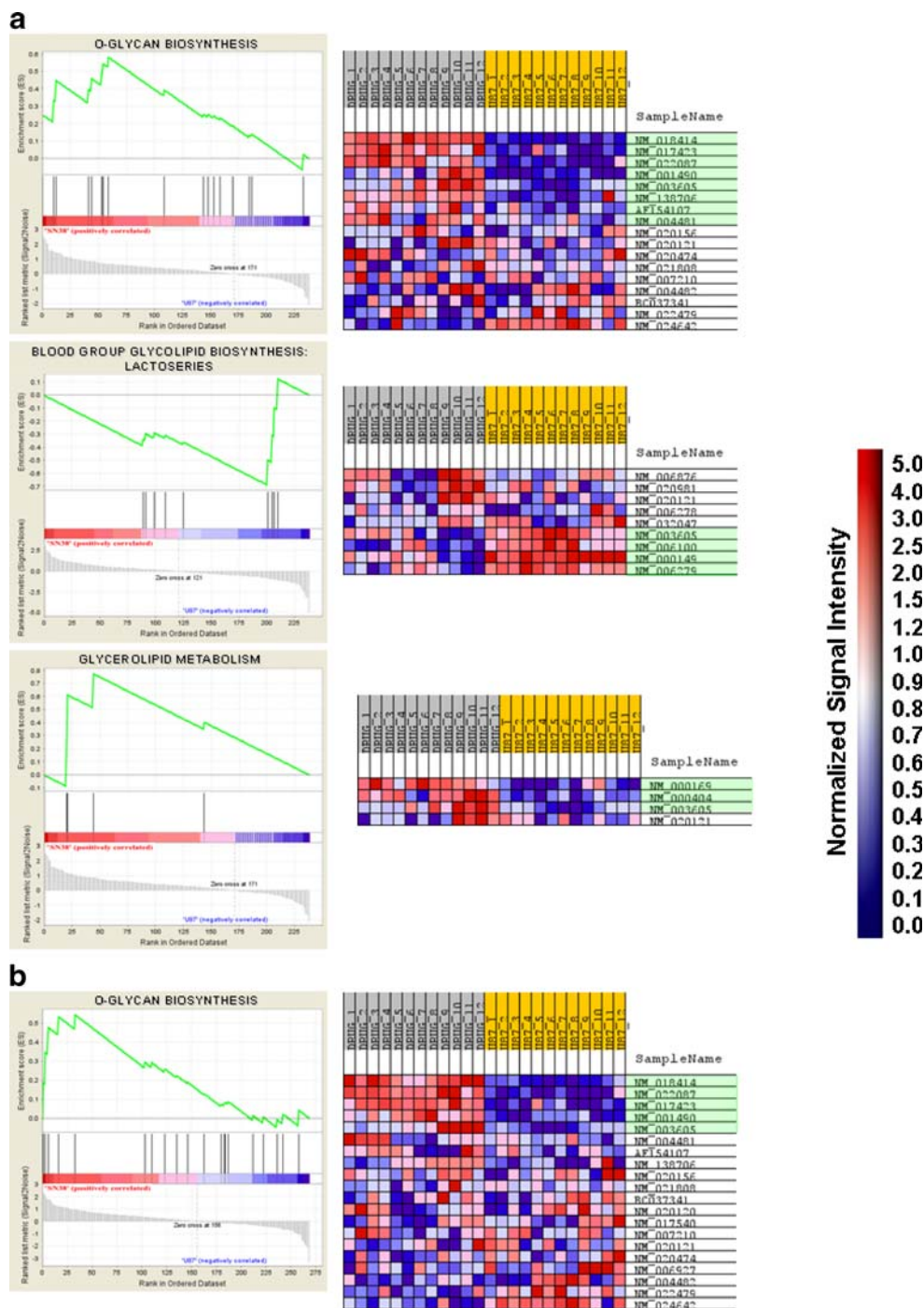
We found that short-chain sulfatides were the most highly modulated class of polar lipid. Sulfatide is a glycosphingolipid with a polar head (galactosyl-3-O-sulfate) and a variable ceramide tail. Fatty acid chain length, degree of unsaturation and hydroxylation determine the manner in which sulfatides and GSLs interact with binding partners. Nonhydroxylated fatty acids are more mobile in membranes and increase membrane fluidity [44]. Membrane fluidity governed by polar head group and phospholipid composition can affect both the orientation and the lateral mobility of membrane constituents. The role of membrane fluidity in cellular presentation of galectin-1 may facilitate the clustering of cell surface receptors, including T cell glycoprotein counter-receptors [45], that actively participate in galectin-1-induced cell death. In our study, only hydroxylated sulfatide (34:1) was detected in untreated U87 MG cells. Treatment with Ad-p53 followed by SN-38, or in reverse order, led to an increase in all sulfatides. The former treatment resulted in the largest-fold increase. Treatment with empty vector followed by SN-38 resulted in expression of long-chain sulfatide. Long chain sulfatide is a prominent component of myelin, produced by oligodendrocytes. Short-chain sulfatide dominates in murine astrocytes and neurons (Isaac *et al.*, 2006) and rat cerebellum [46]. In a recent report, exogenous supplementa-

tion of sulfatide in neuroblastoma cell cultures led to accumulation of sulfatide, ceramide and sphingosine in a time- and dose-dependent manner [47]. Apoptosis of neuroblastoma cells was observed in parallel with the intracellular accumulation of sulfatide and ceramide. Thus, a possible mechanism for sulfatide-induced apoptosis may be the generation of ceramide from sulfatide or the accumulation of sulfatide in lysosomes.

In addition to the differential sulfatide profiles, glyco-transcriptome analyses revealed distinct p53-dependent glyco-gene expression fingerprints in the SN-38 treated cells. Additionally, GSEA analyses of the samples that displayed the highest level of sulfatide modulation (*i.e.*, when wt p53 treatment preceded SN-38 treatment) revealed significant enrichment of the coordinate expression of genesets related to glyco- and glycerolipid metabolic pathways. In neither treatment paradigm, however, was the expression of the two individual enzymes related to sulfatide metabolism, namely arylsulfatase A and galactosylceramide sulfotransferase, altered. However, upregulation of β -galactosidase, an enzyme that can hydrolyze sulfatide, was actually observed in cells treated with wild-type p53 followed by SN-38. The increases in endosomal ceramide observed in sulfatide-induced neuroblastoma apoptosis described above have actually been demonstrated to be due to β -galactosidase activity that directly hydrolyses sulfatide to ceramide without a prior desulfation step [47]. These data strongly suggest that post-transcriptional regulation of sulfatide metabolism is likely responsible for the observed SN-38-mediated alterations in sulfatide levels. The explanation of how glycan diversity on a genome-wide level (via nanoLC-MS/MS analyses) is regulated as a function of its biosynthesis (via glycotranscriptomics), however, remains challenging. We believe that datasets such as the ones generated in this study will help toward the development of computational tools to begin to address such questions.

Changes in the lipid composition of two GSLs, GM1b and GD1, were associated with wt p53 therapy. We did not detect changes in the amounts of hydroxylated or unsaturated lipids, but did observe a reduction in long-chain GM1b and GD1 glycolipids. The differences in length and unsaturation of the fatty acids can affect the cellular

Fig. 4 Enrichment plots for statistically significant gene sets identified by GSEA. Glycogene sets enriched following SN-38 treatment in p53+ background (a) and in a p53- background (b) are depicted. *Black bars* illustrate the position of the probe sets in the context of all of the glycoprobes on the array. The running enrichment score plotted as a function of the position of the ranked list of array probes is shown in *green*. The rank list metric shown in gray illustrates the correlation between the signal-to-noise values of all individually ranked genes according to the class labels (experimental conditions). The genes overrepresented on the leftmost side of the enrichment plots (*i.e.*, O-glycan biosynthetic and glycerolipid metabolic genes) are those that correlate to differential expression in the SN38-treated cells. In contrast, the genes overrepresented on the rightmost side of the enrichment plots (*i.e.*, lactoseries glycolipid biosynthesis) are those that are enriched in the U87 cells. Significantly enriched data sets are defined at a $p < 0.01$ and a false discovery rate (FDR) < 0.25 . The expression profiles of the individual genes within each probe set that contribute to the normalized enrichment score are shown in the *right panel*, with the subset of these genes comprising the leading edge of the gene set highlighted in *green*



localization of gangliosides and the exposure of the three-dimensional epitope of the carbohydrate head group [48, 49]. Relatively higher amounts of hydroxy-fatty acids have been reported in tumor gangliosides [50]. It is unclear whether the reduction of longer chain lipids in GM1 and GD1 in response to wt p53 therapy is caused by decreased synthesis, increased catabolism, or a combination of both.

In contrast, wt p53 therapy led to a relative increase in all classes of phospholipids measured (phosphatidylinositols, phosphatidyl serines, phosphatidyl glycerols and

phosphatidylethanolamines). Similar trends were observed in each class, especially increases in hydroxylated species. Earlier studies on glycolipid function in model membranes that contain phospholipids have demonstrated that the orientation of the carbohydrate relative to the membrane may change when the fatty acid or phospholipid acyl chain length is altered [51–54].

In conclusion, the mammalian lectin, galectin-1, appears to be an important cell-surface glycoprotein in glioma function based on both *in vitro* studies manipulating its

expression with therapeutic agents, its high expression at the invasive edges of glioma cells in a xenograft mouse model, and the positive correlation with its expression and poor patient survival, among others. Since galectin-1 binds to galactose moieties found on both glycoproteins and glycolipids, the studies reported here were undertaken to look at polar lipids as well as the transcriptome associated with glycosylation (*e.g.*, the glycome) under conditions that are known to have important therapeutic implications for the treatment of gliomas and to affect galectin-1 expression. In particular, sulfatide levels were found to increase significantly upon therapeutic treatment. Further, glycomic analysis revealed that those genes associated with sulfatide biosynthesis were not changed, although the galactosidase associated with sulfatide catabolism was significantly increased. Taken together these results support the hypothesis that increases in sulfatide expression play a role in modulating the induction of glioma apoptosis by therapeutic agents—particularly increasing levels of wt p53 and treatment with topoisomerase-1 inhibitor, Irinotecan (or its metabolite SN-38). It is also reasonable to hypothesize that sulfatides may play a role in modulating galectin-1 function as well. The use of the human glioma cell line U87 appears to be an excellent model system both in tissue culture and in intracranial murine xenograft models to further characterize the role of sulfatides in modulating glioma responsiveness to therapeutic agents and the mechanisms that underlie galectin-1 expression and function in gliomagenesis and invasivity.

Acknowledgements Financial support from the National High-Field Fourier Transform Ion Cyclotron Resonance Mass Spectrometry ICR Facility at the National High Magnetic Field Laboratory (NSF DMR 06-54118) and The John C. Merchant Foundation; Live Well, Love Life, Laugh Hard Foundation and the Falk Foundation are also gratefully acknowledged.

References

- Lang, F.F., Shono, T., Gilbert, M.R.: Ad-p53 sensitizes wild-type p53 gliomas to the topoisomerase I inhibitor SN-38. *Neuro Oncol* **4**, 323–324 (2002)
- Puchades, M., Nilsson, C.L., Emmett, M.R., Aldape, K.D., Ji, Y., Lang, F.F., Liu, T.J., Conrad, C.A.: Proteomic investigation of glioblastoma cell lines treated with wild-type p53 and cytotoxic chemotherapy demonstrates an association between galectin-1 and p53 expression. *J Proteome Res* **6**, 869–875 (2007)
- Elad-Sfadia, G., Haklai, R., Ballan, E., Gabius, H.J., Kloog, Y.: Galectin-1 augments Ras activation and diverts Ras signals to Raf-1 at the expense of phosphoinositide 3-kinase. *J Biol Chem* **277**, 37169–37175 (2002)
- Rotblat, B., Niv, H., Andre, S., Kaltner, H., Gabius, H.J., Kloog, Y.: Galectin-1(L11A) predicted from a computed galectin-1 farnesyl-binding pocket selectively inhibits Ras-GTP. *Cancer Res* **64**, 3112–3118 (2004)
- Camby, I., Belot, N., Lefranc, F., Sadeghi, N., de Launoit, Y., Kaltner, H., Musette, S., Darro, F., Danguy, A., Salmon, I., Gabius, H.J., Kiss, R.: Galectin-1 modulates human glioblastoma cell migration into the brain through modifications to the actin cytoskeleton and levels of expression of small GTPases. *J Neuropathol Exp Neurol* **61**, 585–596 (2002)
- Kopitz, J., von Reitzenstein, C., Burchert, M., Cantz, M., Gabius, H.J.: Galectin-1 is a major receptor for ganglioside GM1, a product of the growth-controlling activity of a cell surface ganglioside sialidase, on human neuroblastoma cells in culture. *J Biol Chem* **273**, 11205–11211 (1998)
- Dbaibo, G.S., Pushkareva, M.Y., Rachid, R.A., Alter, N., Smyth, M.J., Obeid, L.M., Hannun, Y.A.: p53-dependent ceramide response to genotoxic stress. *J Clin Invest* **102**, 329–339 (1998)
- Bektas, M., Spiegel, S.: Glycosphingolipids and cell death. *Glycoconj J* **20**, 39–47 (2004)
- Bieberich, E.: Integration of glycosphingolipid metabolism and cell-fate decisions in cancer and stem cells: review and hypothesis. *Glycoconj J* **21**, 315–327 (2004)
- d’Azzo, A., Tessitore, A., Sano, R.: Gangliosides as apoptotic signals in ER stress response. *Cell Death Differ* **13**, 404–414 (2006)
- Hawkins, P.T., Anderson, K.E., Davidson, K., Stephens, L.R.: Signalling through Class I PI3Ks in mammalian cells. *Biochem Soc Trans* **34**, 647–662 (2006)
- Segui, B., Andrieu-Abadie, N., Jaffrezou, J.P., Benoist, H., Levade, T.: Sphingolipids as modulators of cancer cell death: potential therapeutic targets. *Biochim Biophys Acta* **1758**, 2104–2120 (2006)
- Hakomori, S., Handa, K.: Glycosphingolipid-dependent cross-talk between glycosynapses interfacing tumor cells with their host cells: essential basis to define tumor malignancy. *FEBS Lett* **531**, 88–92 (2002)
- Ono, M., Hakomori, S.: Glycosylation defining cancer cell motility and invasiveness. *Glycoconj J* **20**, 71–78 (2004)
- Dawson, G., Moskal, J.R., Dawson, S.A.: Transfection of 2, 6 and 2, 3-sialyltransferase genes and GlcNAc-transferase genes into human glioma cell line U-373 MG affects glycoconjugate expression and enhances cell death. *J Neurochem* **89**, 1436–1444 (2004)
- Furukawa, K., Hamamura, K., Aixinjueluo, W., Furukawa, K.: Biosignals modulated by tumor-associated carbohydrate antigens: novel targets for cancer therapy. *Ann N Y Acad Sci* **1086**, 185–198 (2006)
- Yamamoto, H., Oviedo, A., Sweeley, C., Saito, T., Moskal, J.R.: Alpha 2,6-sialylation of cell-surface N-glycans inhibits glioma formation *in vivo*. *Cancer Res* **61**, 6822–6829 (2001)
- Yamamoto, H., Swoger, J., Greene, S., Saito, T., Hurh, J., Sweeley, C., Leestma, J., Mkrdichian, E., Cerullo, L., Nishikawa, A., Ihara, Y., Taniguchi, N., Moskal, J.R.: Beta 1,6-N-acetylglucosamine-bearing N-glycans in human gliomas: implications for a role in regulating invasivity. *Cancer Res* **60**, 134–142 (2000)
- Forrester, J.S., Milne, S.B., Ivanova, P.T., Brown, H.A.: Computational lipidomics: a multiplexed analysis of dynamic changes in membrane lipid composition during signal transduction. *Mol Pharmacol* **65**, 813–821 (2004)
- Majerus, P.W., Connolly, T.M., Bansal, V.S., Inhorn, R.C., Ross, T.S., Lips, D.L.: Inositol phosphates: synthesis and degradation. *J Biol Chem* **263**, 3051–3054 (1988)
- He, H., Conrad, C.A., Nilsson, C.L., Ji, Y., Schaub, T.M., Marshall, A.G., Emmett, M.R.: Method for lipidomic analysis: p53 expression modulation of sulfatide, ganglioside, and phospholipid composition of U87 MG glioblastoma cells. *Anal Chem* **79**, 8423–8430 (2007)
- Bielawski, J., Szulc, Z.M., Hannun, Y.A., Bielawska, A.: Simultaneous quantitative analysis of bioactive sphingolipids by high-performance liquid chromatography-tandem mass spectrometry. *Methods* **39**, 82–91 (2006)

23. Kim, H.Y., Wang, T.C., Ma, Y.C.: Liquid chromatography/mass spectrometry of phospholipids using electrospray ionization. *Anal Chem* **66**, 3977–3982 (1994)
24. Schwudke, D., Hannich, J.T., Surendranath, V., Grimard, V., Moehring, T., Burton, L., Kurzchalia, T., Shevchenko, A.: Top-down lipidomic screens by multivariate analysis of high-resolution survey mass spectra. *Anal Chem* **79**, 4083–4093 (2007)
25. Hoffman, R.C., Jennings, L.L., Tsigelny, I., Comoletti, D., Flynn, R.E., Sudhof, T.C., Taylor, P.: Structural characterization of recombinant soluble rat neuroligin 1: mapping of secondary structure and glycosylation by mass spectrometry. *Biochemistry* **43**, 1496–1506 (2004)
26. Kroes, R.A., Dawson, G., Moskal, J.R.: Focused microarray analysis of glyco-gene expression in human glioblastomas. *J Neurochem* **103**(Suppl 1), 14–24 (2007)
27. Lee, P.D., Sladek, R., Greenwood, C.M., Hudson, T.J.: Control genes and variability: absence of ubiquitous reference transcripts in diverse mammalian expression studies. *Genome Res* **12**, 292–297 (2002)
28. Schaub, T.M., Hendrickson, C.L., Horning, S., Quinn, J.P., Senko, M.W., Marshall, A.G.: High-performance mass spectrometry: Fourier transform ion cyclotron resonance at 14.5 Tesla. *Anal Chem* **80**, 3985–3990 (2008)
29. Churchill, G.A.: Fundamentals of experimental design for cDNA microarrays. *Nat Genet* **32**(Suppl), 490–495 (2002)
30. Kanehisa, M., Goto, S., Kawashima, S., Okuno, Y., Hattori, M.: The KEGG resource for deciphering the genome. *Nucleic Acids Res* **32**, D277–280 (2004)
31. James, C.G., Ulici, V., Tuckermann, J., Underhill, T.M., Beier, F.: Expression profiling of Dexamethasone-treated primary chondrocytes identifies targets of glucocorticoid signalling in endochondral bone development. *BMC Genomics* **8**, 205 (2007)
32. Li, Z., Srivastava, S., Yang, X., Mittal, S., Norton, P., Resau, J., Haab, B., Chan, C.: A hierarchical approach employing metabolic and gene expression profiles to identify the pathways that confer cytotoxicity in HepG2 cells. *BMC Syst Biol* **1**, 21 (2007)
33. Subramanian, A., Tamayo, P., Mootha, V.K., Mukherjee, S., Ebert, B.L., Gillette, M.A., Paulovich, A., Pomeroy, S.L., Golub, T.R., Lander, E.S., Mesirov, J.P.: Gene set enrichment analysis: a knowledge-based approach for interpreting genome-wide expression profiles. *Proc Natl Acad Sci U S A* **102**, 15545–15550 (2005)
34. Vivanco, I., Palaskas, N., Tran, C., Finn, S.P., Getz, G., Kennedy, N.J., Jiao, J., Rose, J., Xie, W., Loda, M., Golub, T., Mellinghoff, I.K., Davis, R.J., Wu, H., Sawyers, C.L.: Identification of the JNK signaling pathway as a functional target of the tumor suppressor PTEN. *Cancer Cell* **11**, 555–569 (2007)
35. Marshall, A.G., Hendrickson, C.L., Jackson, G.S.: Fourier transform ion cyclotron resonance mass spectrometry: a primer. *Mass Spectrom Rev* **17**, 1–35 (1998)
36. Senko, M.W., Hendrickson, C.L., Emmett, M.R., Shi, S.D., Marshall, A.G.: External accumulation of ions for enhanced electrospray ionization Fourier transform ion cyclotron resonance mass spectrometry. *J Am Soc Mass Spectrom* **8**, 970–976 (1997)
37. Delacour, D., Gouyer, V., Zanetta, J.P., Drobecq, H., Leteurtre, E., Grard, G., Moreau-Hannedouche, O., Maes, E., Pons, A., Andre, S., Le Bivic, A., Gabius, H.J., Manninen, A., Simons, K., Huet, G.: Galectin-4 and sulfatides in apical membrane trafficking in enterocyte-like cells. *J Cell Biol* **169**, 491–501 (2005)
38. Di Paolo, G., De Camilli, P.: Phosphoinositides in cell regulation and membrane dynamics. *Nature* **443**, 651–657 (2006)
39. Chang, G.H., Barbaro, N.M., Pieper, R.O.: Phosphatidylserine-dependent phagocytosis of apoptotic glioma cells by normal human microglia, astrocytes, and glioma cells. *Neuro Oncol* **2**, 174–183 (2000)
40. Hansen, G.H., Immerdal, L., Thorsen, E., Niels-Christiansen, L., Nystrom, B.T., Demant, E.J., Danielsen, E.M.: Lipid rafts exist as stable cholesterol-independent microdomains in the brush border membrane of enterocytes. *J Biol Chem* **276**, 32338–32344 (2001)
41. Li, N., Shaw, A.R., Zhang, N., Mak, A., Li, L.: Lipid raft proteomics: analysis of in-solution digest of sodium dodecyl sulfate-solubilized lipid raft proteins by liquid chromatography-matrix-assisted laser desorption/ionization tandem mass spectrometry. *Proteomics* **4**, 3156–3166 (2004)
42. Chung, C.D., Patel, V.P., Moran, M., Lewis, L.A., Miceli, M.C.: Galectin-1 induces partial TCR zeta-chain phosphorylation and antagonizes processive TCR signal transduction. *J Immunol* **165**, 3722–3729 (2000)
43. Fortin, S., Le Mercier, M., Camby, I., Spiegl-Kreinecker, S., Berger, W., Lefranc, F., and Kiss, R.: Galectin-1 is implicated in the protein kinase C epsilon/vimentin-controlled trafficking of integrin-beta1 in glioblastoma cells. *Brain Pathol* (2008)
44. Vos, J.P., Lopes-Cardozo, M., Gadella, B.M.: Metabolic and functional aspects of sulfogalactolipids. *Biochim Biophys Acta* **1211**, 125–149 (1994)
45. He, J., Baum, L.G.: Presentation of galectin-1 by extracellular matrix triggers T cell death. *J Biol Chem* **279**, 4705–4712 (2004)
46. Pember, Z., Richter, K., Mansson, J.E., Nygren, H.: Sulfatide with different fatty acids has unique distributions in cerebellum as imaged by time-of-flight secondary ion mass spectrometry (TOF-SIMS). *Biochim Biophys Acta* **1771**, 202–209 (2007)
47. Zeng, Y., Cheng, H., Jiang, X., Han, X.: Endosomes and lysosomes play distinct roles in sulfatide-induced neuroblastoma apoptosis: potential mechanisms contributing to abnormal sulfatide metabolism in related neuronal diseases. *Biochem J* **410**, 81–92 (2008)
48. Kannagi, R., Nudelman, E., Hakomori, S.: Possible role of ceramide in defining structure and function of membrane glycolipids. *Proc Natl Acad Sci U S A* **79**, 3470–3474 (1982)
49. Lingwood, C.A.: Aglycone modulation of glycolipid receptor function. *Glycoconj J* **13**, 495–503 (1996)
50. Ladisch, S., Sweeley, C.C., Becker, H., Gage, D.: Aberrant fatty acyl alpha-hydroxylation in human neuroblastoma tumor gangliosides. *J Biol Chem* **264**, 12097–12105 (1989)
51. Nyholm, P.G., Pascher, I.: Orientation of the saccharide chains of glycolipids at the membrane surface: conformational analysis of the glucose-ceramide and the glucose-glyceride linkages using molecular mechanics (MM3). *Biochemistry* **32**, 1225–1234 (1993)
52. Nyholm, P.G., Pascher, I.: Steric presentation and recognition of the saccharide chains of glycolipids at the cell surface: favoured conformations of the saccharide-lipid linkage calculated using molecular mechanics (MM3). *Int J Biol Macromol* **15**, 43–51 (1993)
53. Stewart, R.J., Boggs, J.M.: Dependence of the surface expression of the glycolipid cerebroside sulfate on its lipid environment: comparison of sphingomyelin and phosphatidylcholine. *Biochemistry* **29**, 3644–3653 (1990)
54. Stewart, R.J., Boggs, J.M.: A carbohydrate-carbohydrate interaction between galactosylceramide-containing liposomes and cerebroside sulfate-containing liposomes: dependence on the glycolipid ceramide composition. *Biochemistry* **32**, 10666–10674 (1993)